Pharm Res (2012) 29:1854–1865
DOI 10.1007/s11095-012-0709-5

RESEARCH PAPER

Simultaneously Improving the Mechanical Properties, Dissolution Performance, and Hygroscopicity of Ibuprofen and Flurbiprofen by Cocrystallization with Nicotinamide

Shing Fung Chow • Miles Chen • Limin Shi • Albert H. L. Chow • Changquan Calvin Sun

Received: 20 October 2011 / Accepted: 10 February 2012 / Published online: 23 February 2012

ABSTRACT

Purpose To be fully exploitable in both formulation and manufacturing, a drug cocrystal needs to demonstrate simultaneous improvement of multiple key pharmaceutical properties over the pure drug crystal. The present work was aimed at investigating such feasibility with two model profen-nicotinamide cocrystals.

Methods Phase pure 1:1 ibuprofen-nicotinamide and flurbiprofen-nicotinamide cocrystals were prepared from solutions through rapid solvent removal using rotary evaporation, and characterized by DSC, PXRD, FTIR, phase solubility measurements, equilibrium moisture sorption analysis, dissolution testing and tabletability analysis.

Results Temperature-composition phase diagrams constructed from DSC data for each profen and nicotinamide crystal revealed the characteristic melting point of the 1:1 cocrystal as well as the eutectic temperatures and compositions. Both cocrystals exhibited higher intrinsic dissolution rates than the corresponding profens. The cocrystals also sorbed less moisture and displayed considerably better tabletability than the individual profens and nicotinamide.

Conclusions Phase behaviors of 1:1 profen-nicotinamide cocrystal systems were delineated by constructing their temperature-composition phase diagrams. Cocrystallization with nicotinamide can simultaneously improve tableting behavior, hygroscopicity, and dissolution performance of ibuprofen and flurbiprofen. This could pave the way for further development of such cocrystal systems into consistent, stable, efficacious and readily manufacturable drug products.

KEY WORDS crystal engineering · dissolution · pharmaceutical cocrystal · solubility · tabletability

INTRODUCTION

A long sought goal in pharmaceutical formulation development is the precise and predictive control of the physicochemical properties of active pharmaceutical ingredients (APIs) and pharmaceutical excipients for improving the *in vivo* delivery, storage stability, and manufacturability of drug substances (1). To this end, rational crystal structure design or crystal engineering appears to hold considerable promise (2,3) .

Various strategies for manipulating the solid state of pharmaceutical materials have been attempted to address specific drug formulation problems. For instance, crystallizing APIs into either salts or hydrates has been routinely used in the pharmaceutical industry to enhance the solubility or stability of problematic drugs. However, salt formation is not feasible for neutral molecules and generally unsuitable for weakly ionized compounds due to their severely limited capability for proton transfer. Moreover, many hydrates have been shown to undergo undesired phase transformation during manufacturing and storage (4–6). In cases where neither salt formation nor hydrate formation is suitable or possible, cocrystallization may serve as a viable alternative

S. F. Chow • A. H. L. Chow (✉)
School of Pharmacy, The Chinese University of Hong Kong
Rm 616, Basic Medical Sciences Building
Shatin, N.T. Hong Kong, SAR, China
e-mail: albert-chow@cuhk.edu.hk

M. Chen • L. Shi • C. C. Sun
Department of Pharmaceutics
Pharmaceutical Materials Science & Engineering Laboratory
College of Pharmacy, University of Minnesota
Minneapolis, Minnesota, USA

C. C. Sun (✉)
College of Pharmacy, University of Minnesota
9-127B Weaver-Densford Hall, 308 Harvard street S.E.
Minneapolis, Minnesota 55455, USA
e-mail: sunx0053@umn.edu

means for developing new crystal forms to combat solubility or stability problem. The attractiveness of cocrystallization lies in its broad applicability and high flexibility in designing crystal structures with advantageous solid-state properties. It is generally thought that molecules possessing hydrogen bond donors, acceptors or both, as exemplified by most pharmaceutical compounds, tend to form cocrystals readily. Previous studies have independently demonstrated that cocrystal systems of specific drugs can each be used to address a particular pharmaceutical problem in solubility, dissolution rate (7,8), physical stability (9), bioavailability (10), tabletability (11), or crystal polymorphism (12,13). However, it remains to be shown whether a single cocrystal system can be utilized to concurrently improve several key pharmaceutical properties of a drug substance, including solubility, dissolution, moisture sorption, and mechanical properties. The present study was aimed to investigate such potential multiple utility of a single cocrystal formulation with two model cocrystal systems, namely, ibuprofen–nicotinamide and flurbiprofen–nicotinamide.

R,S-Ibuprofen (IBU) [2-(4-isobutylphenyl) propanoic acid] and flurbiprofen (FLU) [2-(2-fluorobiphenyl-4-yl) propanoic acid] are non-steroidal anti-inflammatory drugs (NSAIDs) (Fig. 1) widely used for their anti-inflammatory, antipyretic and analgesic properties in the treatment of arthritis, fever, and analgesia. Recent studies have indicated that these two NSAIDs may also be of benefits to the treatment of Alzheimer's disease (AD) due to their demonstrated abilities to retard the deterioration of cognitive functions, decrease the incidence of AD, and provide neuroprotection (14–16). As IBU and FLU belong to Class II drugs under the Biopharmaceutics Classification System (BCS), their bioavailabilities are severely limited by their low aqueous solubilities and dissolution rates. It has been previously established that these two profens are capable of forming cocrystals with nicotinamide (NCT; Fig. 1) through hydrogen bonding between the pyridine group of NCT and the carboxylic acid group of the profens (17). NCT is the amide of niacin belonging to the vitamin B family (B_3). Apart from being readily water-soluble and chemically compatible with either profen, NCT has demonstrated an ability to restore cognition in AD transgenic mice through sirtuin inhibition and selective reduction of Thr231-Phosphotau (18). Thus the co-formulation of IBU or FLU with NCT in the form of a cocrystal may offer additional or even synergistic therapeutic benefits in the treatment of AD.

MATERIALS AND METHODS

Materials

R,S-Ibuprofen (IBU) and flurbiprofen (FLU) (purity >99.9%) were purchased from Yick-Vic Chemicals & Pharmaceuticals Ltd. (Hong Kong, China) Nicotinamide (NCT) was purchased from Sigma Aldrich (St. Louis, MO, USA). All organic solvents used were of HPLC or analytical grade and were purchased from RCI Labscan Ltd. and Merck KGaA. All chemicals and solvents were used as received. Water used was double-distilled.

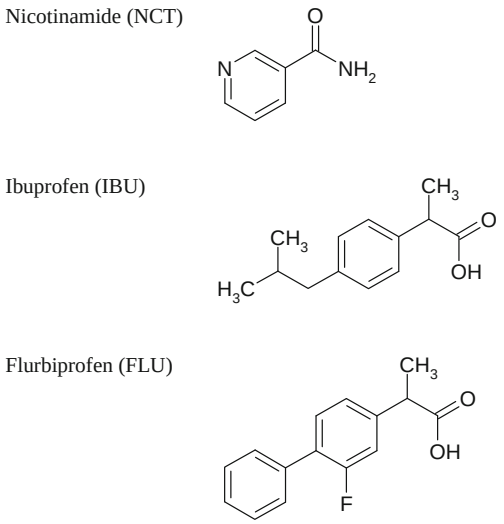

Fig. 1 Chemical structures of cocrystal formers.

Preparation of Cocrystals

Cocrystal samples were prepared by dissolving equivalent mole fractions of IBU or FLU and NCT in ethanol. The solution was filtered through 0.22 μm membrane filters prior to rapid removal of the solvent under vacuum using a rotary evaporator (Buchi, Germany). The resulting product was dried in an oven (40°C) for 3 h and gently triturated with mortar and pestle to a fine powder prior to analyses. As a reference for comparison, an undersaturated solution of equivalent molar concentrations of each profen and NCT was prepared and allowed to dry on a petri dish by slow evaporation at ambient conditions. The crystallized product was collected and similarly dried at 40°C and triturated before characterization.

Thermal Analyses

DSC and TGA profiles were generated respectively with a differential scanning calorimeter (Pyris 1, PerkinElmer Corporation, USA) and thermogravimetric analyzer (TGA 7, Perkin Elmer Corporation, USA). All measurements were performed at least thrice and analyzed using Pyris manager software.

High purity indium was used to calibrate the DSC instrument prior to the analysis. For the DSC measurements, accurately weighed samples (3–5 mg) were placed in hermetically sealed aluminum pans and heated through the

corresponding melting temperature range at a scan speed of 1°C/min. In TGA experiments, each sample (5–7 mg) was placed on an open pan and heated at 10°C/min from 50°C to 350°C. Nitrogen was used as the purge gas at 20 mL/min for both DSC and TGA analyses.

Powder X–Ray Diffraction (PXRD)

PXRD patterns were collected with a powder X–ray diffraction system (Model PW 1830, Philips, Almelo, The Netherlands). Sample was carefully packed into an aluminum holder of about 2 mm thickness. The measurements were conducted using a 3 kW Cu anode (λ=1.54056 Å) over a 2θ interval of 2° to 40° at a step size of 0.02° (2θ) and a dwell time of 2 s per step.

Fourier-Transform Infrared Spectroscopy

A Fourier-Transform Infrared (FTIR) spectrophotometer (Spectrum BX, MA, USA) was used in KBr diffuse reflectance mode for recording the IR spectra of the samples. A total of 64 scans were performed (with a 4 cm^{-1} resolution) over the range of 4,000–650 cm^{-1} at an interval of 2 cm^{-1} for each sample. Data were collected and analyzed by the built-in software.

Solubility Determination

Excess amount of each starting material (IBU, FLU, NCT) was placed in four 10 mL screw capped test tubes containing 1 mL of deionized water, ethanol, ethyl acetate, and acetone respectively. The suspensions were stirred with magnetic stirring bars at 20°C for 72 h prior to filtration through 0.22 μm membrane filters. The collected filtrates were then diluted with ethanol to an appropriate concentration for HPLC analysis while the filtered residues were analyzed by DSC and PXRD to check for potential phase conversion during equilibration in the various solvents.

Stability Constant Determination

Determination of the stability constants (K_s) of the two profen-NCT complexes in water employed the method of Higuchi *et al.* (19) with modifications. Briefly, excess IBU or FLU was equilibrated in water with different concentrations of NCT under mild agitation at 20°C for 72 h. The resulting suspension was then filtered and the filtrate was analyzed by HPLC for the profen and NCT concentrations. A phase solubility plot of profen concentration *versus* NCT concentration in solution was constructed and K_s was calculated from the slope and intercept of the plot based on a 1:1 stoichiometric complex formation, as confirmed by DSC.

Intrinsic Dissolution Rate Measurements

Using a custom-made stainless steel die, each powder was compressed into a pellet (6.39 mm in diameter) against a flat stainless steel disc under 1000 lb force for 2 min. Following compression, the visually smooth pellet surface was coplanar with the surface of the die (verified using a microscope at × 50 magnifications). While rotating at 300 rpm, the die was immersed in 500 mL de-ionized water at 37°C in a water jacketed beaker. Absorbance of light was continuously monitored using a UV-vis fiber optic probe (Ocean Optics, Dunedin, FL) connected to a computer. Absorbance data were converted into concentrations using a calibration curve, constructed using the same setup, to obtain concentration–time profiles. Finally, intrinsic dissolution rate was calculated from the slope of the initial linear portion of the dissolution curve and the pellet surface area exposed to the dissolution medium.

High Performance Liquid Chromatography (HPLC)

The concentrations of IBU, FLU and NCT in solutions were determined at ambient temperature using an HPLC system (Waters 2695, equipped with a photodiode array detector) and a 10×4.6 mm Hypersil® BDS 5 μm C_{18} column (Thermo Hypersil Ltd., Cheshire, UK). The mobile phase, consisting of acetonitrile (A) and 0.01% (v/v) trifluoroacetic acid in water (B), was eluted under the following gradient conditions: 0–3.0 min, 20%A; 3.0–11.5 min, 80%A; 11.5–15.0 min, 20%A. The flow rate was set at 1 mL/min and absorbance was measured at 217 nm. The injection volume was ten-microliter.

Moisture Sorption Measurement

Moisture sorption of samples was measured at 20°C as a function of relative humidity as previously reported by Tong *et al.* (2008) with slight modifications (20). Distilled water (100% RH) and various saturated solutions of inorganic salts, viz., phosphorous pentoxide (0% RH), lithium chloride (11% RH), potassium acetate (23% RH), magnesium chloride (33% RH), potassium carbonate (43% RH), sodium nitrite (65% RH), sodium chloride (75% RH), potassium chloride (85% RH), potassium nitrate (92.5% RH), were employed to maintain different relative humidities, or water activities, for construction of moisture sorption isotherms. Samples were accurately weighed (120–150 mg) on petri dishes and placed in sealed glass jars containing the aforementioned aqueous systems. Equilibrium water content was recorded if successive sample weight measurements did not differ by more than ±0.1 mg. At the end of the study, samples were checked by DSC and TGA for potential phase changes during the equilibration period. The moisture

sorption data were fitted to the Brunauer-Emmett-Teller (BET) equation (Eq. 1) using a non-linear curve fitting software (SigmaStat v 3.5):

$$W = \frac{W_m C\left(\frac{P}{P^o}\right)}{\left[1-\left(\frac{P}{P^o}\right)\right]\left[1-\left(\frac{P}{P^o}\right)+C\left(\frac{P}{P^o}\right)\right]} \quad (1)$$

where W is the moisture content (g/100 g dried powder) at a defined relative vapor pressure (P/P^o), water activity or relative humidity (% RH); W_m is the theoretical monolayer moisture content; and C is an equilibrium or affinity constant related to the heat of adsorption. As with most moisture sorption analysis for Type II isotherm, only the data points up to 43% RH were used in the present analysis (21).

Powder Compaction Analysis

Since the as-received raw materials differed significantly in both particle size and morphology, the materials were first triturated by means of a mortar and pestle to minimize possible effects of these variables on powder compaction properties (22,23). The triturated powders were then allowed to relax for at least a week prior to tabletability study. Potential phase changes during the relaxation period were ruled out by PXRD. Approximately 250–300 mg of powder was manually filled into a tableting die and compressed at predetermined pressures (12.5–300 MPa) using a universal material testing machine (model 1485, Zwick, Germany). Compression speed was set at 1 mm/min. Both punches and die cavity were lubricated by coating with a thin layer of 5% (wt%) magnesium stearate suspended in ethanol followed by air drying. Tablets (flat-faced, 8 mm diameter) were allowed to relax overnight before their weights, diameters and thickness were measured. Tablets were then fractured diametrically using a Texture Analyzer (TA-XT2i, Texture Technologies Corp., NY, USA) at a testing speed of 0.01 mm/s. Maximum breaking force, tablet diameter, and tablet thickness were used to calculate tensile strength according to Eq. 2.

$$\sigma = \frac{2F}{10^6 \cdot \pi \cdot D \cdot T} \quad (2)$$

where σ is tensile strength (MPa), F is the breaking force (N), D is the tablet diameter (m), and T is the thickness of tablet (m). Tabletability profiles were obtained by plotting tensile strength as a function of compaction pressure. Environmental conditions were 7–10% RH and 24°C throughout the compaction study.

RESULTS

Powder X-Ray Diffraction Patterns

The phase purity of the cocrystal samples prepared by rapid solvent evaporation and simple evaporation techniques was examined by PXRD based on the presence or absence of the characteristic peaks of the corresponding individual components [i.e., IBU (6.2° 2θ), FLU (10.8° 2θ) and NCT (14.85° 2θ)], as shown in Fig. 2. The PXRD pattern of IBU–NCT cocrystal obtained by slow evaporation had the characteristic peaks of IBU and NCT at 6.2° and 14.85° respectively while the sample prepared by rapid solvent evaporation showed the characteristic peaks for the cocrystal at 3.3° and 12.65° 2θ but no peak indicative of either IBU or NCT. FLU–NCT cocrystal behaves similarly to IBU–NCT cocrystal, where rapid evaporation generated pure cocrystal characterized by major peaks at 6.55°, 9.75°and 12.95° 2θ.

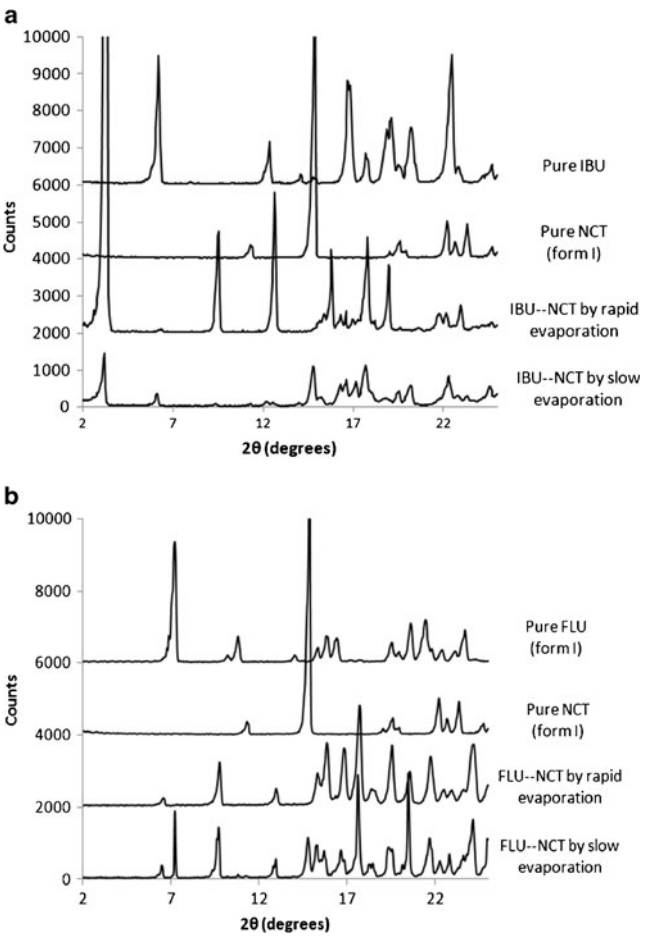

Fig. 2 PXRD patterns showing the effects of evaporation rate on cocrystal formation between IBU (FLU) and NCT. Solids produced by rapid evaporation were nearly pure cocrystals while a mixture of IBU, NCT, and their cocrystals were produced by slow evaporation. (**a**) IBU and NCT; (**b**) FLU and NCT.

Temperature-Composition Phase Diagrams

Presented in Fig. 3a and b are the temperature-composition phase diagrams of the IBU–NCT and FLU–NCT systems constructed by thermal analysis of corresponding binary mixtures at various compositions using DSC. Key thermal data are tabulated in Table I. For the IBU–NCT system, a local maximum melting temperature of 89.9°C (ΔH_f= 45.4 kJ/mol, at mole fraction of 0.5) was observed. This is significantly different from the melting temperatures of IBU (71.7°C) and NCT (126.9°C), and accords with that of a previously reported 1:1 cocrystal of racemic ibuprofen with NCT (24). The two eutectics formed at 64.7°C and 86.9°C, corresponding to the 0.19 and 0.59 mole fraction of NCT, respectively. On the other hand, the FLU–NCT cocrystals melted at 96.4°C (ΔH_f=47.0 kJ/mol, at mole fraction 0.5) and the eutectics occurred at 86.0°C and 93.7°C, respectively.

The melting point of the FLU–NCT cocrystal determined in our study was approximately 23°C higher than that reported for a new phase (73.4°C) produced by the same cocrystal formers from Kofler hot-stage melting experiments (17). PXRD analysis of the Kofler melt material has also revealed the presence of the metastable FLU Form III (17), which melts at 87°C (25). Although different polymorphs of FLU-NCT cocrystal could exhibit different melting points, it is more likely that eutectic melting between FLU Form III and cocrystal led to an observation of melting at 73.4°C. The surprising kinetic stability of the supposedly very unstable FLU Form III in the Kofler melt material also suggests the possible presence of chemical impurities, which not only stabilize FLU Form III but also depress the melting point of the crystals.

Table I Key Thermal Properties of Cocrystal Formers and Cocrystals (n=3)

Sample	T_m (°C)	ΔH_f (kJ/mol)	Onset temp. of weight loss
IBU	71.7 ± 0.2	27.2 ± 0.4	205.5 ± 0.5
FLU	109.3 ± 0.2	28.9 ± 0.5	213.0 ± 0.9
NCT	126.9 ± 0.3	23.3 ± 0.3	249.8 ± 0.8
IBU–NCT	89.9 ± 0.2	45.4 ± 0.8	207.5 ± 0.9
FLU–NCT	96.4 ± 0.2	47.0 ± 1.6	224.9 ± 1.6

Thermal Stability

The IBU–NCT cocrystal exhibited a melting point between those of IBU and NCT (Fig. 4a). In contrast, the melting of

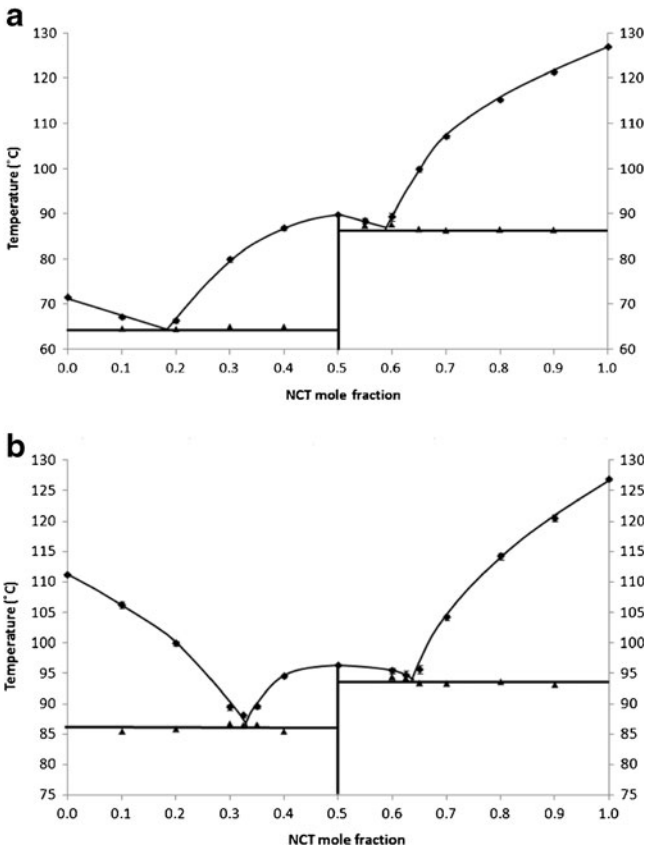

Fig. 3 Melting point phase diagrams of **a**) IBU–NCT and **b**) FLU–NCT cocrystal systems (n=3).

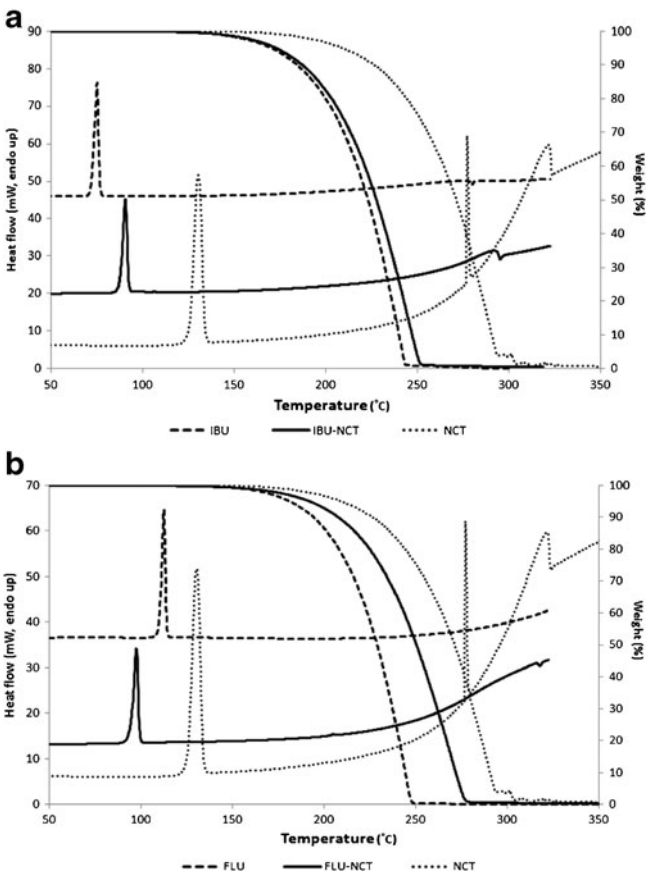

Fig. 4 Thermal stability of the two profen–NCT cocrystals determined by DSC and TGA, **a**) IBU–NCT and **b**) FLU–NCT.

FLU–NCT occurred at a temperature (96.3°C) below those of FLU (111.7°C) and NCT (126.9°C) (Fig. 4b). However, the molar enthalpies of both cocrystals were considerably higher than those of their individual components (Table I). The onset temperatures for weight losses of different melts are summarized in Table I.

Fourier-Transform Infrared Spectral Characteristics

The FTIR spectra for both IBU–NCT and FLU–NCT cocrystal systems are shown in Fig. 5a and b, respectively. In the IBU–NCT cocrystal, two broad peaks were identified at 2,490 cm^{-1} and 1,982 cm^{-1}. In addition, spectral peak shifts were observed for various polar functional groups, as summarized in Table II. The FLU–NCT cocrystal similarly showed two broad peaks in the same IR region and characteristic peak shifts for the polar groups (Table II).

Solubility and Intrinsic Dissolution Rate

The solubility data of IBU, FLU and NCT in water and various organic solvents are tabulated in Table III. The

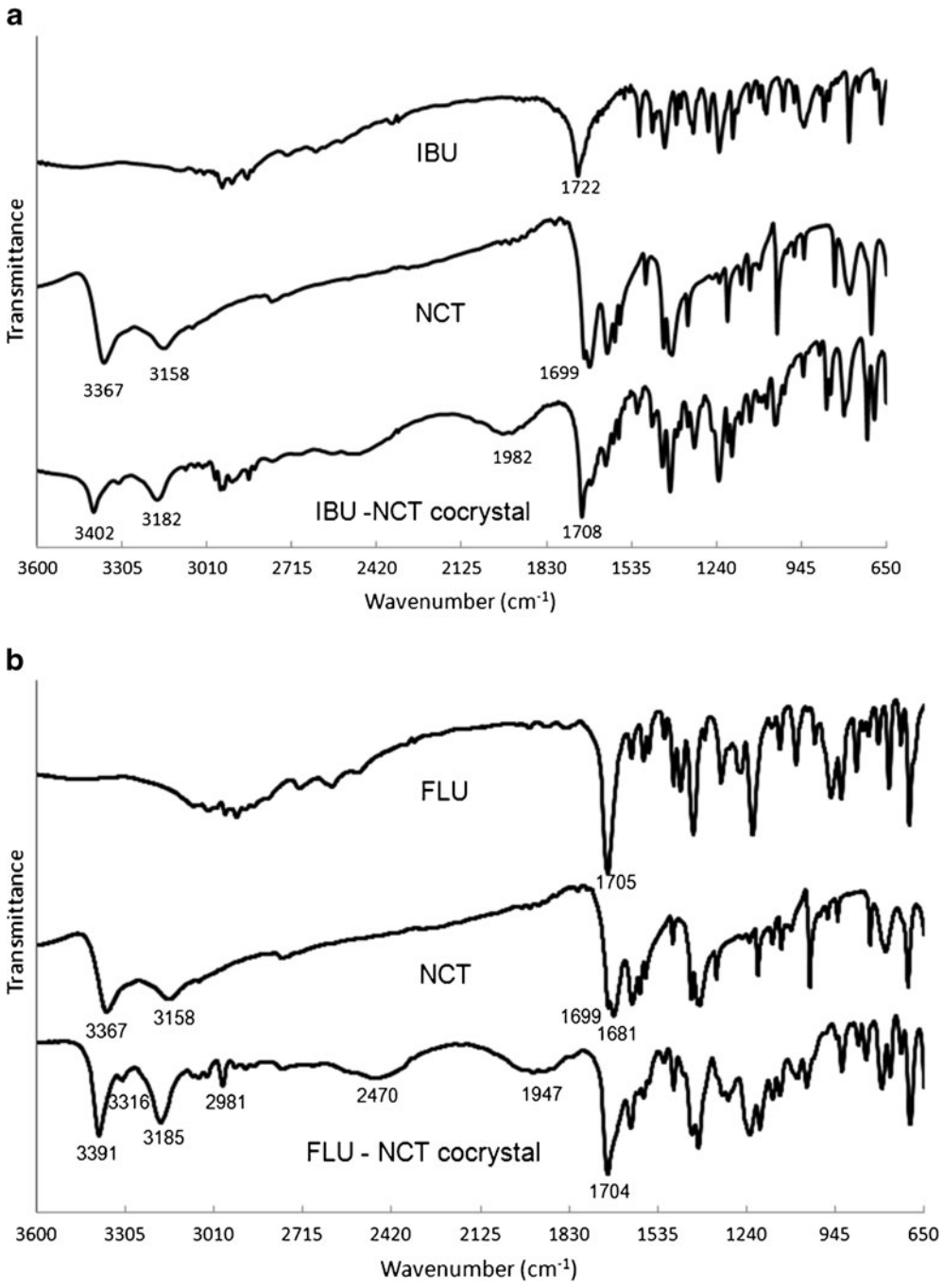

Fig. 5 FTIR spectra of (**a**) IBU–NCT and (**b**) FLU–NCT cocrystal systems.

Table II Key Features in the FTIR Spectra of Cocrystal Formers and Cocrystals

Peak assignment	NCT (cm^{-1})	IBU (cm^{-1})	IBU–NCT (cm^{-1})	FLU (cm^{-1})	FLU–NCT (cm^{-1})
ν (NH_2)	3,367	–	3,402	–	3,391
	3,158		3,182		3,185
ν (C=O)	1,681	1,722	1,708	1,705	1,704
δ (NH_2)	1,619	–	1,624	–	1,624
ν (OH)	–	3,050–2,500	3,050–2,500	3,050–2,500	3,050–2,500
ν $(CN)_{amide}$	1,395	–	1,401	–	1,400
Intermolecular O•••H—N (H-bond)	–	–	3,316	–	3,316
Intermolecular O—H•••N (H-bond)	–	–	2,490 and 1,982	–	2,470 and 1,947
Fingerprint region (for cocrystals)	–	–	857, 797 and 717		868,841 and 791

solubilities of the two cocrystals could not be determined since they were readily converted back to their respective profens during equilibration in water, as discussed earlier. Phase solubility studies were conducted according to the method of Higuchi *et al.* (19) to determine the stability constant, K_s, of the two profen–NCT complexes (Fig. 6). The phase solubility plots of both systems revealed a typical A_L type complexation behavior where the concentration of IBU or FLU increased linearly with the concentration of NCT. Based on the formation of a 1: 1 molecular complex (as confirmed by DSC and PXRD), the K_s values of IBU–NCT and FLU–NCT were determined to be 0.0949 and 0.0967 M^{-1}, respectively.

Attempts were also made to determine the K_s values of both cocrystal systems by equilibrating excess amounts of the cocrystals in water containing different concentrations of NCT according to the method of Nehm *et al.* (26). However, this approach has not been successful since both cocrystals readily dissociate back to the parent profens irrespective of the NCT concentration in water (as evidenced by HPLC and PXRD analysis of the sediment collected from the aqueous medium after the study). Consequently, instead of obtaining a curvilinear decreasing trend in profen concentration with increasing NCT concentration (as expected from the suppression of dissociation), an essentially linear increase in profen concentration with NCT concentration similar to the Higuchi's phase solubility plot was observed.

Table III Equilibrium Solubilities of Cocrystal Formers at 20°C (n=3)

Chemical Species	Solubility (mM) (± SD)			
	Water	Ethanol	Ethyl acetate	Acetone
IBU	0.201 ± 0.003	2,575 ± 12	2,303 ± 4	2,881 ± 19
FLU	0.095 ± 0.002	1,254 ± 6	924 ± 22	1,806 ± 28
NCT	4,956 ± 73	1,201 ± 9	103 ± 2	802 ± 17

Presented in Table IV are the intrinsic dissolution rate data. At 37°C, NCT showed very rapid dissolution in water, consistent with its high aqueous solubility (Table III). However, both profens displayed very low dissolution rates.

Moisture Sorption

Figure 7 shows that the moisture sorption profiles of the two cocrystals and their individual formers roughly followed Type II isotherms. All the samples displayed a steady increase in moisture sorption up to 92.5% RH, beyond which an upsurge in water uptake was observed for the cocrystals and NCT. Below 92.5% RH, both cocrystals sorbed less water than their respective profens and NCT. Additionally, the sorbed moisture did not induce any solid phase changes or dissociation of the cocrystals, as attested by DSC analysis (data not shown). To enable quantitative comparison between samples, the moisture sorption isotherms were analyzed by the BET model within the RH range of 0–43.5% and the parameters obtained by nonlinear regression are presented in Table V. The data fitting for all isotherms was excellent with an R^2 value of ~0.99, indicative of the general adequacy of the BET model for describing the sorption data in the RH range of interest. In addition, the computed parameter estimates were all stable with the exception of the C value for the IBU sample which displayed a significantly larger standard error (p=0.148). Such parameter instability is prone to occur in the present data treatment where barely enough data points (n=4) are fitted to a 2-parameter mathematical model.

Tabletability

Except for FLU, tablet tensile strength generally increased monotonically with increasing compaction pressure (Fig. 8a and b). For FLU, tablet tensile strength increased with increasing pressure only up to 150 MPa. Further increase

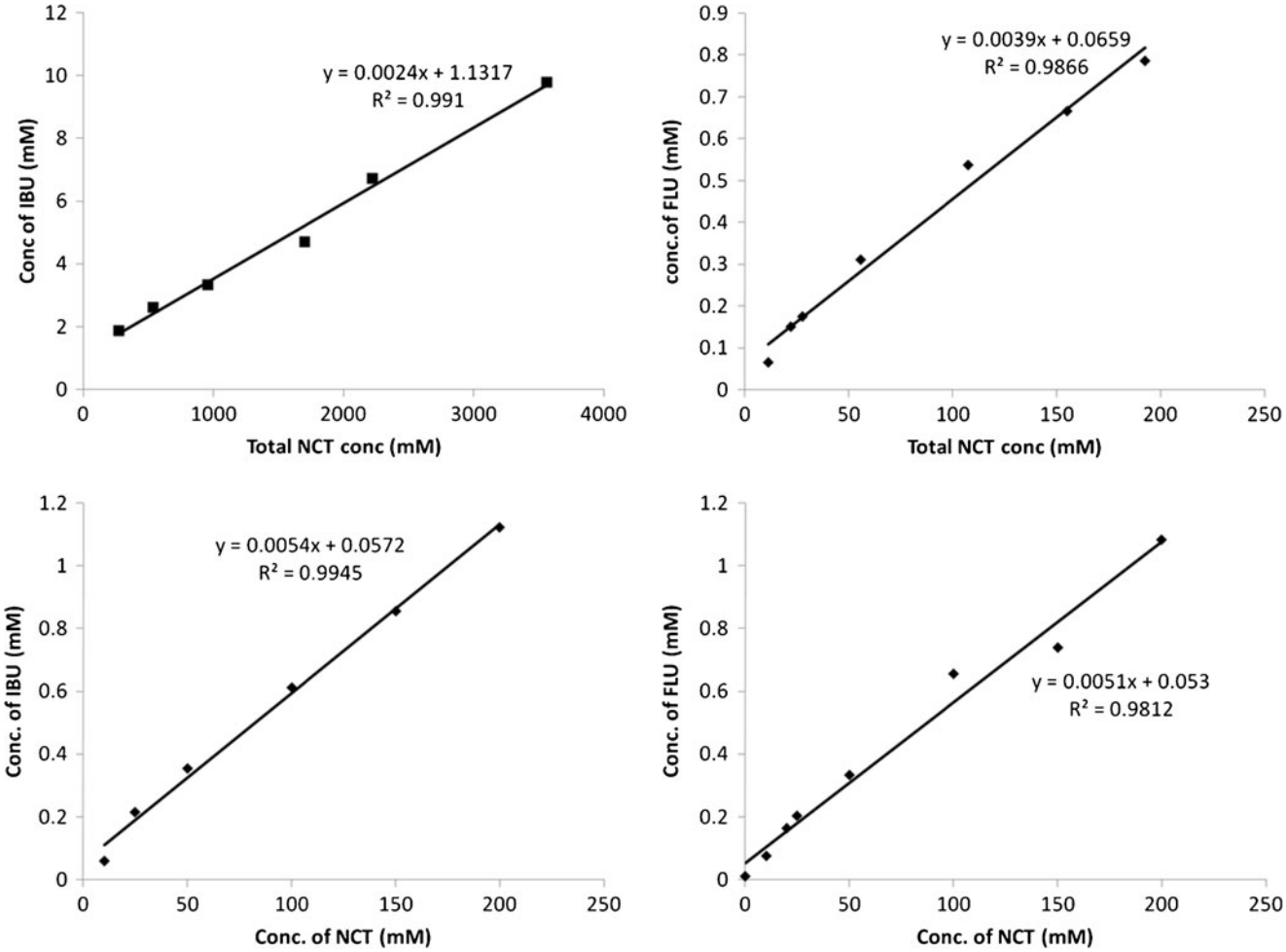

Fig. 6 Phase solubility diagrams for cocrystals constructed using Nehm's method (*top*, starting with excess cocrystal) and Higuchi's method (*bottom*, starting with excess profens).

in compaction pressure led to a sharp reduction in tensile strength (Fig. 8a), which coincides with the increase in tablet porosity in the same pressure range (150–300 MPa) (Fig. 9). Defect lines roughly parallel to table surfaces were visible for tablets prepared at 250 MPa and 300 MPa. Only one intact tablet could be made at 300 MPa due to severe lamination of tablets.

Table IV Intrinsic Dissolution Rates of Cocrystal Formers and Cocrystals at 37°C in Water (n=3)

	Intrinsic dissolution rate	
	$\mu g\ cm^{-2}\ min^{-1}$	$\mu M\ m^{-2}\ min^{-1}$
IBU	23.6 ± 2.7	1,145 ± 131
FLU	7.1 ± 0.4	289 ± 16
NCT	62,193 ± 729	5,092,360 ± 59,695
IBU–NCT	181.1 ± 7.0	5,514 ± 213
FLU–NCT	35.2 ± 1.4	962 ± 38

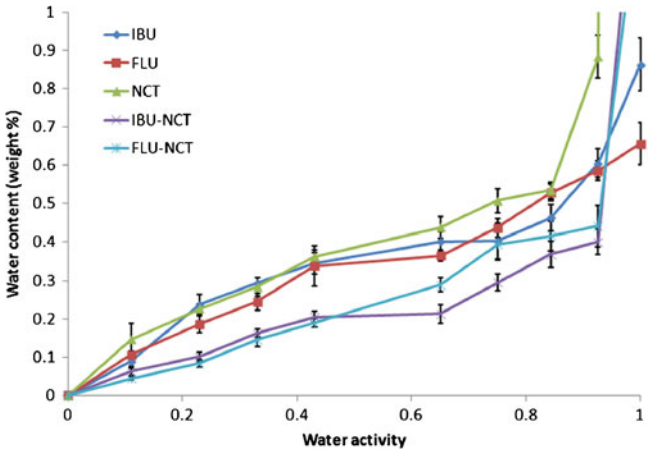

Fig. 7 Moisture sorption isotherms of the profen–NCT cocrystals and their individual formers at 20°C.

Table V BET Parameters Obtained from Nonlinear Regression Analysis Using SigmaStat

Samples	W_m (g/100 g)	*p* value	*C*	*p* value	R^2
IBU	0.254 (0.036)	0.006	5.71(2.95)	0.148	0.987
FLU	0.234 (0.035)	<0.001	4.91 (0.73)	0.007	0.998
NCT	0.232 (0.003)	<0.001	10.2 (0.68)	<0.001	1.000
IBU–NCT	0.158 (0.013)	0.001	3.89 (0.93)	0.025	0.997
FLU–NCT	0.173 (0.019)	0.003	2.28 (0.57)	0.028	0.997

Mean values from triplicate measurements were employed in BET model fitting. Values in parentheses depict standard errors of the parameter estimates

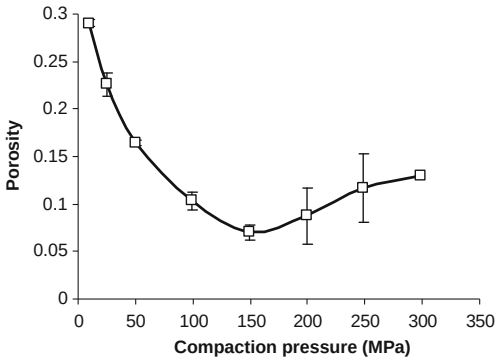

Fig. 9 Porosity profile of FLU is approximately a mirror image of its tabletability profile.

DISCUSSION

Phase Purity and Stability

An examination of the PXRD patterns of cocrystal formers (IBU, FLU and NCT) and corresponding cocrystals (IBU–NCT and FLU–NCT) showed that high-purity cocrystals were only obtainable by rapid solvent removal using rotary evaporation but not by the slow evaporation technique (Fig. 2). Thus, it would appear that rapid solvent evaporation favors only the formation of the cocrystal nuclei and hence a pure solid phase while slow evaporation tends to generate mixed nuclei of NCT, profen, and cocrystal, and consequently an impure sample. The latter may be attributable to the creation of localized regions of uneven supersaturation in the unstirred solution, particularly near the solution surface where evaporation occurs, thereby triggering the nucleation of all three different solid phases. The PXRD patterns of both IBU–NCT and FLU–NCT cocrystals in this study agree well with those in the literature (17).

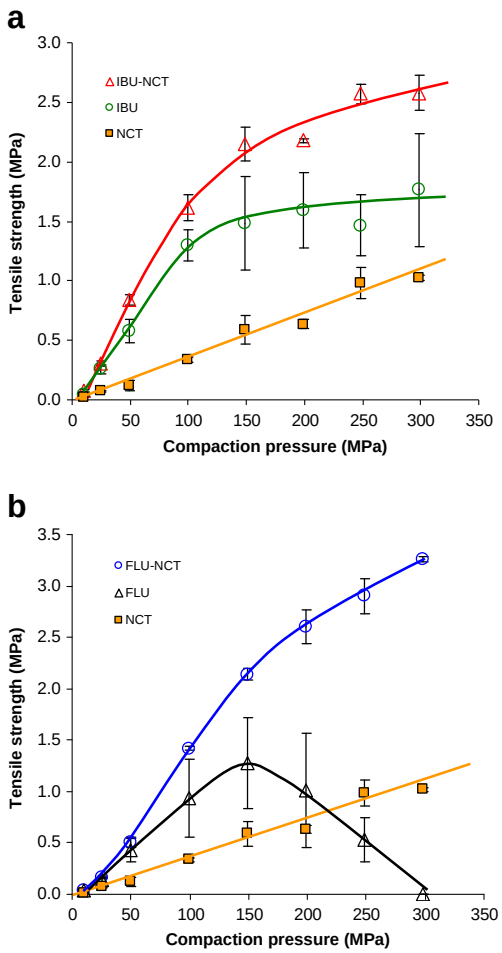

Fig. 8 Tabletability of the profen–NCT cocrystals and their individual formers. (**a**) IBU–NCT system; (**b**) FLU–NCT system.

An essential knowledge for any cocrystal system is the temperature-composition phase diagram which indicates the phases formed at different compositions of the cocrystal formers over a range of temperatures. For a binary mixture forming a 1: 1 cocrystal, a typical phase diagram shows three local melting point maxima (i.e., for the two pure components and cocrystal), separated by two eutectics (27). Such a representative phase diagram has been demonstrated for the two profen–NCT cocrystals in the present study (Fig. 3). The higher melting point of the IBU–NCT cocrystal relative to pure IBU reflects a higher thermal stability while the lower melting point of the FLU–NCT cocrystal compared to pure FLU suggests a potential for undesired melting of the material when being processed (Table I).

Hydrogen bonding is generally known to play an important role in the formation of profen–NCT cocrystals, which has been substantiated by the FTIR data in the present study (Table II). For the two cocrystal systems, two broad absorption peaks in the range of 1900–2500 cm^{-1} characteristic of intermolecular O-H•••N hydrogen bond (28) are clearly evident (Fig. 5). Spectral peak shifts have also been observed for the amino, carbonyl, hydroxyl, and amide

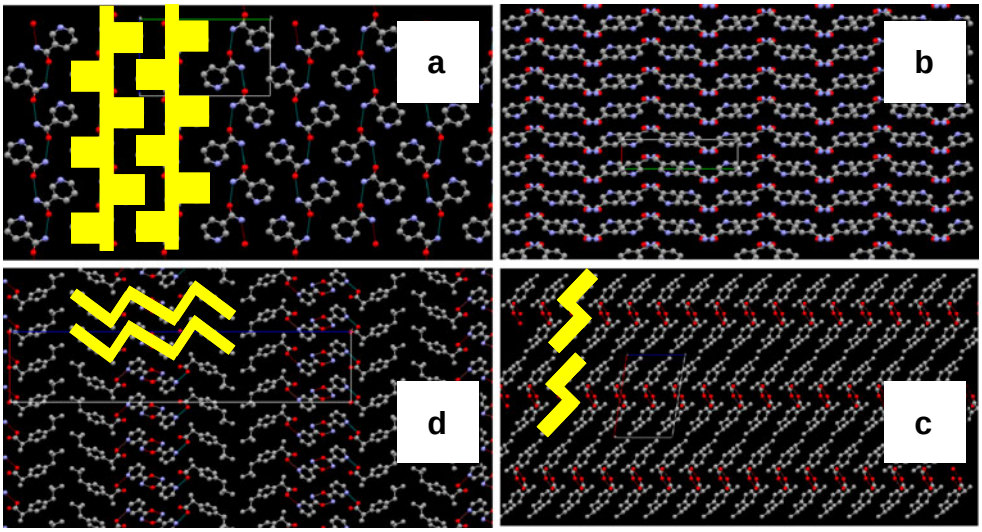

Fig. 10 Crystal packing patterns of (**a**) NCT (viewed along *a* axis); (**b**) NCT viewed along *c* axis. (**c**) IBU (viewed along *b* axis); (**d**) IBU–NCT cocrystal (viewed along *a* axis).

groups, reflecting their involvement in the hydrogen bonding between the cocrystal formers (Table II).

Despite their good thermal stability in the solid state, both cocrystals readily dissociate back to their individual components during equilibration in aqueous media, as reflected by their extremely low K_s values in water (Fig. 6). Similar instability in water has also been reported for the phenobarbitone–nicotinamide system in previous studies (29). In fact, it has been demonstrated that cocrystals composed of highly water-soluble coformers (>10 mg/mL) are prone to rapid dissociation in water (30), which may be ascribed to the considerably stronger interaction between the coformer and water than that between the coformer and drug. This is probably the case for the profen–NCT systems in the present study where NCT has an aqueous solubility of ~4.96 M at ambient conditions (Table III), which is far in excess of 10 mg/mL (0.08 M).

Moisture Sorption

While the two cocrystals are physically unstable in aqueous solutions, they tend to sorb less moisture than the individual cocrystal formers (particularly NCT) at ambient RH (Fig. 7), reflecting their relatively non-hygroscopic nature. Similar phenomenon has also been reported for the indomethacin–saccharin cocrystal (7). Based on the computed *C* values (i.e., affinity constants for water vapor adsorption) in Table V, the relative resistance of the samples to moisture sorption follows the order: FLU–NCT > IBU–NCT > FLU > IBU > NCT. As expected, NCT is the most hygroscopic, displaying the strongest affinity for water vapor. Cocrystallization with the hydrophobic former, IBU or FLU, substantially reduces the moisture sorption tendency of NCT by 2.5 and 4 fold respectively. The cocrystals also exhibit a 1.5 and 2 fold reduction in affinity for moisture than IBU and FLU respectively. This confirms that cocrystal formation is useful in reducing the hygroscopicity of these substances, therefore, potentially benefiting their future processing.

The differences in water solubility and hygroscopicity of the various samples can be explained in terms of their crystal structures and associated intermolecular interactions (notably hydrogen bonding). NCT possesses an amide group and a pyridine ring with a basic nitrogen, both of which can readily interact with water via hydrogen bonding, thus accounting for its good water solubility. In the solid state, the amide groups of individual NCT molecules are all involved in intermolecular hydrogen bonding leaving the pyridine nitrogens free to interact with the environmental water vapor molecules (Fig. 10a), thus contributing to its hygroscopic nature. However, in the cocrystal form with IBU or FLU, all the pyridine nitrogens of NCT form hydrogen bonds with the carboxylic hydrogens of the profen (Fig. 10d) and are therefore not available for bonding with water, resulting in a decrease in moisture sorption at relatively low RHs. However, as the RH was raised beyond 92.5%, the deliquescent relative humidity (DRH) of NCT was eventually reached (31), as evidenced by an abrupt surge in water uptake for both NCT and NCT-containing cocrystals (Fig. 7). Structurally, FLU differs from IBU in having a phenyl group in place of an isobutyl group in addition to a fluoro substituent on the benzene ring at the C-2 position of the propanoic acid (Fig. 1), which renders FLU more hydrophobic than IBU. This structural difference, coupled with the fact that the carboxylic groups of individual profen molecules are all tied up in intermolecular hydrogen bonds (Fig. 10c), possibly accounts for the lower affinity of FLU crystal for moisture sorption. Cocrystallization of IBU or FLU with NCT results in a stronger crystal lattice, possibly via extensive hydrogen bonding, as reflected by the higher molar enthalpy of fusion of the resulting cocrystals (Table I). Such lattice strengthening may also contribute to the reduced hygroscopicity of the cocrystals.

Solubility and Dissolution Performance

As mentioned earlier, owing to the rapid dissociation of the profen–NCT cocrystals in water, direct measurement of their aqueous solubility has not been possible. Thus the intrinsic dissolution rate, which is closely related to solubility, was determined instead. As expected for BCS Class II drugs, the two profens exhibit very slow dissolution (Table IV), consistent with their low aqueous solubilities (Table III). However, when forming a cocrystal with NCT, both profens displayed substantial enhancement in their dissolution rates (by ~8 fold for IBU and ~5 fold for FLU; Table IV), indicating substantially higher solubility of the cocrystals than the corresponding profens. This suggests that the cocrystal formation would be an effective means for improving the dissolution-limited *in vivo* delivery of both NSAIDs.

Mechanical Properties

Cocrystallization can either improve or impair compaction properties of drugs (11,32). In the present study, all samples except FLU exhibited a monotonically increasing trend in tablet tensile strength as a function of compaction pressure. For FLU, tablet tensile strength increased with increasing compaction pressure up to a maximum at 150 MPa and decreased thereafter (Fig. 8). Similar behavior has been previously shown for caffeine (11). This phenomenon is known as over-compaction where extensive elastic recovery of tablet during unloading process in the >150 MPa pressure region causes disruption of inter-particulate bonds, resulting in weaker tablets (33,34). Both profen cocrystals display improved tabletability compared with corresponding profen or NCT crystal (Fig. 8). These results imply that the manufacturability of compressed tablets containing both profen and NCT would be better with their cocrystal forms.

The tableting behaviors of the various samples can be explained with reference to their crystal structures. The basic building block of the NCT crystal is a molecular column (Fig. 10a). Along each column, the pyridine rings protrude out to form two rugged edges. Each column runs in opposite direction from its neighbors. Part of each pyridine ring fit in the space in the neighboring column to form a layer. These layers stack to form the three-dimensional crystal structure. In this type of structure, sliding of individual columns is hindered by the neighboring columns. Moreover, sliding between layers is energetically unfavorable due to the unevenness of the layers (Fig. 10b). The absence of facile sliding among adjacent molecular architectures in this crystal determines that its plasticity is low. However, since the neighboring columns are not hydrogen bonded, they can be readily separated by a tensile stress. Consequently the material tends to be brittle (i.e., fractured easily) when stressed, for example, during milling and compaction. This is consistent with the tableting behavior of NCT, where tablet tensile strength increases nearly linearly with compaction pressure, a profile characteristic of brittle materials (Fig. 8a).

In the racemic IBU crystal, hydrogen bonded columns stack into flat layers (Fig. 10c), which is the building unit for the crystal. The NCT–IBU cocrystal (Fig. 10d) is structurally similar to the IBU crystal in the sense that hydrogen bonded molecular columns stack to form flat layers. Plasticity of this type of crystals is expected to be high because of the effective plastic deformation mechanism involving facile sliding between adjacent hydrogen-bonded columns under shear (35). The observation that tablet tensile strength of both crystals gradually levels off with increasing pressure (Fig. 8) is characteristic of the behavior of plastic materials.

Although the observed similarity in both crystal structural features and shape of tabletability plots between IBU and its cocrystal with NCT would suggest comparable plasticity for the two materials, the tabletability of the cocrystal form is apparently higher (Fig. 8). This observation accords with the higher lattice energy or bonding strength of the cocrystal as suggested by its higher enthalpy of fusion (45.4 kJ/mol as opposed to 27.2 kJ/mol for IBU; Table I). Hence, the better tabletability of the cocrystal than IBU is largely a result of its higher bonding strength.

CONCLUSIONS

We have shown, for the first time, that cocrystallization with a water-soluble ingredient (nicotinamide) can simultaneously improve several key pharmaceutical properties including dissolution rate, moisture sorption, and mechanical properties for poorly water-soluble ibuprofen and flurbiprofen. The new information generated in the present study, notably the temperature-composition phase diagram and tableting behavior, could pave the way for further development of such cocrystal systems into high quality drug products.

ACKNOWLEDGMENTS & DISCLOSURES

Financial support from the Chinese University of Hong Kong (research postgraduate studentship and conference travel grant for SFC) is gratefully acknowledged.

REFERENCES

1. Ku MS. Preformulation consideration for drugs in oral CR formulation. In: Wen H, Park K, editors. Oral controlled release

formulation design and drug delivery: Theory to practice. New Jersey: John Wiley & Sons; 2010. p. 47–70.
2. Blagden N, de Matas M, Gavan PT, York P. Crystal engineering of active pharmaceutical ingredients to improve solubility and dissolution rates. Adv Drug Deliv Rev. 2007;59(7):617–30.
3. Desiraju GR. Crystal engineering: The design of organic solids. Amsterdam: Elsevier; 1989.
4. Tong HHY, Chow ASF, Chan HM, Chow AHL, Wan YKY, Williams ID, Shek FLY, Chan CK. Process-induced phase transformation of berberine chloride hydrates. J Pharm Sci. 2010;99(4):1942–54.
5. Khankari RK, Grant DJW. Pharmaceutical hydrates. Thermochim Acta. 1995;248:61–79.
6. Giron D, Grant DJW. Evaluation of solid-state properties of salts. In: Stahl PH, Wermuth CG, editors. Handbook of pharmaceutical salts: Properties, selection, and use. Weinheim: Wiley-VCH; 2008. p. 41–82.
7. Basavoju S, Bostroem D, Velaga SP. Indomethacin-Saccharin cocrystal: design, synthesis and preliminary pharmaceutical characterization. Pharm Res. 2008;25(3):530–41.
8. Shiraki K, Takata N, Takano R, Hayashi Y, Terada K. Dissolution improvement and the mechanism of the improvement from cocrystallization of poorly water-soluble compounds. Pharm Res. 2008;25(11):2581–92.
9. Trask AV, Motherwell WDS, Jones W. Physical stability enhancement of theophylline via cocrystallization. Int J Pharm. 2006;320 (1–2):114–23.
10. McNamara DP, Childs SL, Giordano J, Iarriccio A, Cassidy J, Shet MS, *et al.* Use of a glutaric acid cocrystal to improve oral bioavailability of a low solubility API. Pharm Res. 2006;23(8):1888–97.
11. Sun CC, Hou H. Improving mechanical properties of caffeine and methyl gallate crystals by cocrystallization. Cryst Growth Des. 2008;8(5):1575–9.
12. Lancaster RW, Karamertzanis PG, Hulme AT, Tocher DA, Lewis TC, Price SL. The polymorphism of progesterone: stabilization of a 'disappearing' polymorph by co-crystallization. J Pharm Sci. 2007;96(12):3419–31.
13. Lou B, Bostroem D, Velaga SP. Polymorph control of felodipine form II in an attempted cocrystallization. Cryst Growth Des. 2009;9(3):1254–7.
14. Yip AG, Green RC, Huyck M, Cupples LA, Farrer LA. Nonsteroidal anti-inflammatory drug use and Alzheimer's disease risk: the MIRAGE Study. BMC Geriatr. 2005;5:2.
15. Prasad KN, Cole WC, Prasad KC. Risk factors for Alzheimer's disease: Role of multiple antioxidants, non-steroidal anti-inflammatory and cholinergic agents alone or in combination in prevention and treatment. J Am Coll Nutr. 2002;21(6):506–22.
16. Babiloni C, Frisoni GB, Del Percio C, Zanetti O, Bonomini C, Cassetta E, *et al.* Ibuprofen treatment modifies cortical sources of EEG rhythms in mild Alzheimer's disease. Clin Neurophysiol. 2009;120(4):709–18.
17. Berry DJ, Seaton CC, Clegg W, Harrington RW, Coles SJ, Horton PN, *et al.* Applying hot-stage microscopy to Co-crystal screening: a study of nicotinamide with seven active pharmaceutical ingredients. Cryst Growth Des. 2008;8(5):1697–712.
18. Green KN, Steffan JS, Martinez-Coria H, Sun X, Schreiber SS, Thompson LM, *et al.* Nicotinamide restores cognition in Alzheimer's disease transgenic mice via a mechanism involving sirtuin inhibition and selective reduction of Thr231-phosphotau. J Neurosci. 2008;28(45):11500–10.
19. Higuchi T, Connors KA. Phase-solubility techniques. Advan Anal Chem Instr. 1965;4:117–212.
20. Tong HHY, Wong SYS, Law MWL, Chu KKW, Chow AHL. Anti-hygroscopic effect of dextrans in herbal formulations. Int J Pharm. 2008;363(1–2):99–105.
21. Zhang J, Zografi G. The relationship between "BET" - and "free volume" - derived parameters for water vapor absorption into amorphous solids. J Pharm Sci. 2000;89(8):1063–72.
22. Sun C, Grant DJW. Influence of crystal shape on the tableting performance of L-lysine monohydrochloride dihydrate. J Pharm Sci. 2001;90(5):569–79.
23. Sun C, Grant DJW. Effects of initial particle size on the tableting properties of L-lysine monohydrochloride dihydrate powder. Int J Pharm. 2001;215(1–2):221–8.
24. Friscic T, Jones W. Cocrystal architecture and properties: design and building of chiral and racemic structures by solid-solid reactions. Faraday Discuss. 2007;136:167–78.
25. Henck J, Kuhnert-Brandstaetter M. Demonstration of the terms enantiotropy and monotropy in polymorphism research exemplified by Flurbiprofen. J Pharm Sci. 1999;88(1):103–8.
26. Nehm SJ, Rodriguez-Spong B, Rodriguez-Hornedo N. Phase solubility diagrams of cocrystals are explained by solubility product and solution complexation. Cryst Growth Des. 2006;6 (2):592–600.
27. Davis RE, Lorimer KA, Wilkowski MA, Rivers JH, Wheeler KA, Bowers J. Studies of phase relationships in cocrystal systems. ACA Trans. 2004;39:41–61.
28. Aakeroey CB, Salmon DJ, Smith MM, Desper J. Cyanophenyloximes: reliable and versatile tools for hydrogen-bond directed supramolecular synthesis of cocrystals. Cryst Growth Des. 2006;6 (4):1033–42.
29. Sanghvi R, Evans D, Yalkowsky SH. Stacking complexation by nicotinamide: a useful way of enhancing drug solubility. Int J Pharm. 2007;336(1):35–41.
30. Schultheiss N, Newman A. Pharmaceutical cocrystals and their physicochemical properties. Cryst Growth Des. 2009;9(6):2950–67.
31. Jayasankar A, Good DJ, Rodriguez-Hornedo N. Mechanisms by which moisture generates cocrystals. Mol Pharm. 2007;4 (3):360–72.
32. Chattoraj S, Shi L, Sun CC. Understanding the relationship between crystal structure, plasticity and compaction behaviour of theophylline, methyl gallate, and their 1: 1 co-crystal. Cryst Eng Comm. 2010;12(8):2466–72.
33. Sun CC. Materials science tetrahedron-a useful tool for pharmaceutical research and development. J Pharm Sci. 2009;98 (5):1671–87.
34. Sun CC. Decoding powder tabletability: roles of particle adhesion and plasticity. J Adhes Sci Technol. 2011;25(4–5):483–99.
35. Sun C, Grant DJW. Compaction properties of L-lysine salts. Pharm Res. 2001;18(3):281–6.